

Article

Electric Vehicles Charging Scheduling Strategy Based on Time Cost of Users and Spatial Load Balancing in Multiple Microgrids

Jiaqi Zhang¹, Yongxiang Xia^{1,*}, Zhongyi Cheng¹ and Xi Chen^{2,3}

¹ School of Communication Engineering, Hangzhou Dianzi University, Hangzhou 310018, China; zjqzzz@hdu.edu.cn (J.Z.); horizonczy@hdu.edu.cn (Z.C.)

² China Electric Power Research Institute, Beijing 100192, China; xc@ieee.org

³ GEIRI North America, San Jose, CA 95134, USA

* Correspondence: xiayx@hdu.edu.cn

Abstract: In a sustainable energy system, managing the charging demand of electric vehicles (EVs) becomes increasingly critical. Uncontrolled charging behaviors of large-scale EV fleets will exacerbate loads imbalanced in a multi-microgrid (MMG). At the same time, the time cost of users will increase significantly. To improve users' charging experience and ensure stable operation of the MMG, we propose a new joint scheduling strategy that considers both time cost of users and spatial load balancing among MMGs. The time cost encompasses many factors, such as traveling time, queue waiting time, and charging time. Meanwhile, spatial load balancing seeks to mitigate the impact of large-scale EV charging on MMG loads, promoting a more equitable distribution of power resources across the MMG system. Compared to the Shortest Distance Matching Strategy (SDMS) and the Time Minimum Matching Strategy (TMMS) methods, our approach improves the average peak-to-valley ratio by 9.5% and 10.2%, respectively. Similarly, compared to the Load Balancing Matching Strategy (LBMS) and the Improved Load Balancing Matching Strategy (ILBMS) methods, our approach reduces the average time cost by 31.8% and 25% while maintaining satisfactory spatial load balancing. These results demonstrate that the proposed method achieves good results in handling electric vehicle scheduling problems.

Keywords: electric vehicles; time cost of users; spatial load balancing; load distribution; safe operation



Academic Editor: Vladimir Katic

Received: 30 November 2024

Revised: 15 January 2025

Accepted: 16 January 2025

Published: 19 January 2025

Citation: Zhang, J.; Xia, Y.; Cheng, Z.; Chen, X. Electric Vehicles Charging Scheduling Strategy Based on Time Cost of Users and Spatial Load Balancing in Multiple Microgrids. *World Electr. Veh. J.* **2025**, *16*, 46. <https://doi.org/10.3390/wevj16010046>

Copyright: © 2025 by the authors. Published by MDPI on behalf of the World Electric Vehicle Association. Licensee MDPI, Basel, Switzerland. This article is an open access article distributed under the terms and conditions of the Creative Commons Attribution (CC BY) license (<https://creativecommons.org/licenses/by/4.0/>).

1. Introduction

The increasing use of electric vehicles (EVs) in recent years presents both opportunities and challenges for sustainable development. The demand for EV charging is increasing significantly with the rapid popularity of EVs around the world. Large-scale EV charging demand can generate instantaneous high load impacts on the grid, which can lead to grid instability and even trigger power shortages and blackouts in localized areas. Appropriate scheduling strategies are needed to guide user charging and avoid peak hour power load accumulation as much as possible. Without guidance on EV charging activities, users are more likely to choose the charging station closest to them. Such a large-scale simultaneous charging of EVs tends to cause transient high load at some charging stations. This will undoubtedly aggravate the burden on MMGs during peak electricity consumption, which is not conducive to the safe operation of MMGs [1,2]. On the contrary, EVs possess higher flexibility compared to other types of loads in MMGs [3–5]. If the charging behavior of EV users can be guided by effective strategies, EVs can be turned into a tool to balance the load among MGs, which will significantly reduce the burden they impose on MMGs [6–8].

Therefore, the reliability and efficiency of the EV charging process is ensured by developing a new charging strategy that meets the needs of EV users and balances the load differences between MGs.

EVs scheduling strategies can assign EVs to appropriate charging stations to achieve different optimization objectives. Single-objective optimization problems have been considered from the user's point of view or the grid's point of view. When considering the user's perspective, the focus is on the user's cost during the charging process, such as time cost, economic cost, and so on. Elghitani et al. [9] proposed a way to assign EVs to appropriate charging stations in large-scale EV scenarios, minimizing the average time from requesting charging service to obtaining it for EV users. Li et al. [10] considered the user economic cost based on a road network model with the aim to reduce the charging cost of EVs users.

Xiang et al. [11] performed optimal path planning for users based on road network models for a single vehicle. Ji et al. [12] proposed a personalized fast charging navigation strategy for EVs based on dynamic queuing interaction effects, where a dynamic reservation–waiting queue model was developed. Shi et al. [13] proposed a memory-based ant colony optimization method, which reduces the total waiting time of customers and the transportation cost of online cars. Rasheed et al. [14] proposed a model for calculating fees based on real-time load demand so as to optimize customers' cost and improve their satisfaction. Sweda et al. [15] searched for the least cost path by considering the initial charge level, total travel time and battery life. Jia et al. [16] proposed a two-tier optimization problem considering EV paths and charging planning under capacity constraints to generate charging routes and develop charging schedules that satisfy power constraints. On the other hand, from the MMG perspective, Refs. [17,18] focused on the MMG operation cost and optimized the MMG size, as well as the operation scheduling, to efficiently utilize the resources and minimize the MMG cost. Zhao et al. [19] proposed a hierarchical energy management architecture that coordinates multiple MMGs for effective energy management. Shi et al. [20] proposed a new approach to spatial–temporal multi-graph convolutional network based on an attention mechanism for charging station load forecasting that effectively captured the spatial–temporal relationship between charging stations. In Ref. [21], an efficient valley filling strategy was proposed to coordinate charging to achieve temporal load balancing by utilizing surplus power during low demand hours. Similarly, Kandpal et al. [22] also proposed a day-ahead electric vehicle scheduling strategy to alleviate the phase load imbalance problem. Nimalsiri et al. [23] reduced the peak of the load profile through a Vehicle To Grid (V2G) interaction technique. Chen et al. [24] proposed a Load Balancing Matching Strategy (LBMS) to reduce the load fluctuation of the MMG system by allocating EVs to appropriate charging stations to achieve spatial load balancing. In Ref. [25], the effect of limited service capacity on the LBMS algorithm was considered, and the performance of the LBMS algorithm was improved in Ref. [26].

Furthermore, the EV charging behavior is related to the interests of many parties, such as the users, the power grid, and the operator of charging facilities. Some researchers conducted co-optimization of multiple objectives by considering the interests of multiple parties. Zhang et al. [27] proposed a charging facility planning model that considered not only the impact of new charging facilities on the power system but also the impact of the charging facility location on the transport system and minimized the cost of operating the transport system, as well as the time cost of users. In Ref. [28], dispatch optimization models were proposed to achieve orderly EVs charging so as to reduce charging cost and promote grid stability. Luo et al. [29] optimized the charging station load while considering the level of congestion on the road close to the charging station. Guo et al. [30] minimized the total user charging time and guided the user to choose the charging station with the shortest time on the road. Then, the charging station optimized the charging rate according to the

number of users and the power margin. Ref. [31] proposed a method to optimize the user charging time cost and the MMG power at the same time to achieve spatial load balancing.

As a movable load, an EV has flexible demand response characteristics in the spatial scope. Refs. [24,25] designed charging scheduling strategies to achieve load balancing among MGs. However, they did not take into account the time cost of users. From EV users' perspective, users should experience convenience so that they could accept the strategy. Therefore, from both the user's and MMG's perspectives, we would like to consider the time cost of users, as well as the MMG load balancing, in an integrated manner. In Ref. [31], although both perspectives were considered, the fluctuation of the MMG load during the time period of charging was ignored. In addition, the proposed algorithm required that the allocation information of all vehicles was available in advance. In other words, the algorithm needed the information of vehicles which appear later to determine the dispatch result of current vehicles, which violates causality.

Based on the above problems, we aim to optimize both the user's time cost and the spatial load balancing among MMG system. By recommending the optimal charging stations and planning the optimal paths for vehicles, the time cost of users is reduced, and the spatial load balancing scheduling is coordinated. We develop a new joint scheduling strategy, called Minimum Time Cost–Spatial Load Balancing Matching Strategy (MTC-SLBMS), to meet the traveling needs of EV users, as well as the stable operation of power grids.

The main contributions of this paper are listed as follows:

- (1) By integrating real-time traffic information, as well as charging stations' information and MMG loads' information, this paper proposes a more complete large-scale EVs charging joint scheduling strategy called MTC-SLBMS, which accurately formulates charging navigation strategies for users, reduces user time cost, and optimizes MMG spatial load balancing effects.
- (2) We aim to optimize both the user's time cost and the spatial load balancing degree of MMGs. Compared to the SDMS and TMMS that consider the user's time cost unilaterally, or consider MMGs load balancing unilaterally in the LBMS [24] and ILBMS [26], our strategy has a good starvation effect in both aspects. It provides a more comprehensive and efficient solution for large-scale EVs' charging scheduling and optimizes the overall performance of the system.
- (3) We also explore the performance of the proposed MTC-SLBMS method under different MMG scales, different levels of user participation, and different charging station capacities, and we verify the feasibility of the method in many aspects, making the conclusion more universal.

The remainder of this paper is organized as follows. Section 2 describes in detail the process of calculating the road network model, time cost of users, and MMG average load. The joint scheduling strategy that coordinates the time cost of users with spatial load balancing is presented in Section 3. Section 4 illustrates the effectiveness of the joint scheduling strategy by experimentally comparing it with four different scheduling strategies. We conclude this paper in Section 5 and discuss the limitation and future work.

2. The Description of Model

This section describes the proposed model, detailing its key components, interactions, and underlying assumptions. They form the basis for analysis and validation.

2.1. Multi-Microgrid

The microgrid (MG) is an important part of modern power grids. It is a local energy network composed of a variety of distributed energy resources, energy storage systems, and energy management systems. This network can realize autonomous operation in the

case of disconnecting the main power grid. We assume that all EV charging facilities in an MG are connected to the same charging aggregator and are located at the same network node as the substation or transformer of the MG, as shown in Figure 1. In this way, we assume that there is only one charging station per MG. An MMG is a microgrid cluster that connects multiple microgrids through a physical grid and a communication network, as shown in Figure 2. Each grid represents an MG, and the red circle represents a charging station. MGs are connected by red cables. Thus, the exchange of energy and information between each microgrid can be carried out, and the stability of the power grid can be enhanced through resource sharing and coordinated operation. There are a large amount of EV charging infrastructures in an MMG. If an efficient scheduling strategy is used, a large amount of charging energy demand generated by the EVs can be effectively managed, and the load distribution among MGs can be optimized.

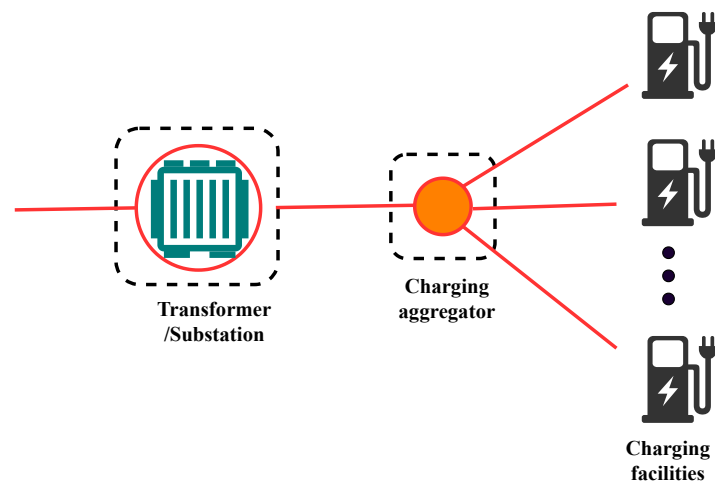


Figure 1. Schematic diagram of charging aggregator in microgrid.



Figure 2. Multi-microgrids.

2.2. Time Cost of Users

This subsection explores the time-related costs incurred by users' charging behaviors, focusing on various factors contributing to their overall time cost.

2.2.1. Cost of Traveling Time on the Road

We first model the traffic network. $G = (V, E, D)$ denotes the traffic network, where V is the set of all road nodes, E is the set of all connected road segments, and D is the set of road weights. In the road network model, the length of the road section is used as the weight of the traffic network; thus, the element D_{ij} in the generated road weighting matrix D is expressed as

$$D_{ij} = \begin{cases} d_{ij}, & e_{ij} \in E \\ 0, & e_{ij} \notin E \text{ and } i = j, \\ \infty, & e_{ij} \notin E \text{ and } i \neq j \end{cases} \quad (1)$$

where d_{ij} denotes the distance from point i to point j . We assume that the roads are all bi-directionally connected, so $d_{ij} = d_{ji}$. When an EV user sends a charging request, the vehicle dispatch center receives the charging request. Based on the information such as the location of EV, the remaining SoC status of the vehicle, and MMG loads after accessing charging, it recommends the most suitable charging station for the user. We assume that EV users are accepting the advice given by the dispatch center to go to the appropriate charging station. The EV does not leave the charging station until it is fully charged. When the n th EV sends a charging request at time t_0 , the initial state of charge (SoC) is $B_{ini,n}^{t_0}$, and the vehicle dispatch center will record the position of the n th EV.

In an urban transport network, an EV's traveling speed is mainly influenced by road capacity and traffic flow. From Ref. [10], the traveling speed $\bar{V}_{ij}(t)$ of the EV on the road section e_{ij} at time t can be expressed as

$$\bar{V}_{ij}(t) = \frac{\bar{V}_{ij}^{free}}{1 + \left(\frac{q_{ij}(t)}{C_{ij}}\right)^\beta}, \quad (2)$$

$$\beta = a + b \left(\frac{q_{ij}(t)}{C_{ij}}\right)^m, \quad (3)$$

where \bar{V}_{ij}^{free} denotes the free-flow speed of the road section e_{ij} ; C_{ij} denotes the capacity of the road section e_{ij} ; $q_{ij}(t)$ denotes the traffic flow of the road section e_{ij} at the moment of t ; and a , b , and m are the adaptive coefficients for different road levels, which can be obtained from the experimental data in Ref. [10]. In our model, roads are divided into urban expressways, main roads, and secondary roads.

Different traffic flows influence vehicle travel speeds. Sometimes, while being the shortest route, its traveling time is not the shortest. The dispatch center will take into account the road traffic conditions and recommend charging stations with the shortest possible traveling time on the road, saving the user's time expenditure in traveling. To address dynamic changes in traffic patterns, we continuously track the location of each electric vehicle, thereby updating the traffic conditions of the current road segments. These real-time data are used to dynamically calculate the travel time for roads, allowing the system to respond quickly based on the latest traffic information. Especially in the case of sudden traffic disruptions, the system can adjust the vehicle's travel route or charging station allocation to maintain optimal performance. Here, we construct a time-weighted matrix T , where T_{ij} denotes the estimated traveling time on the road section connecting nodes i and j . We use the speed-flow model [10] to calculate the traveling speed \bar{V}_{ij} of the vehicle on different road sections, and the traveling time of vehicle on each road section is calculated by the following equation:

$$t_{ij} = \frac{d_{ij}}{\bar{V}_{ij}}. \quad (4)$$

Therefore, the element T_{ij} in the time-weighted matrix T is expressed as

$$T_{ij} = \begin{cases} t_{ij}, & e_{ij} \in E \\ 0, & e_{ij} \notin E \text{ and } i = j. \\ \infty, & e_{ij} \notin E \text{ and } i \neq j \end{cases} \quad (5)$$

In this way, we have the time cost on each road section. We assume that roads are all bi-directionally connected, so we have $t_{ij} = t_{ji}$. Then, using the Floyd algorithm, we substitute the time-weighted matrix T to find the shortest traveling time path between any two nodes. Finally, we generate a sequence of nodes $L_{i,j}$ contained in the shortest path, and $L_{i,j}$ can be represented as

$$L_{i,j} = (k_1, k_2, \dots, k_m). \quad (6)$$

Each node in the sequence $L_{i,j}$ represents a specific road node on the EV's traveling path. $k_1 = i$ is the start node (usually the current location of the EV), and $k_m = j$ is the end node (i.e., the location of the charging station). The distance between the n th vehicle EV and each charging station can be represented by the vector R , which is defined as

$$R = (R_{n,1}, R_{n,j}, \dots, R_{n,N_G}), \quad (7)$$

where $R_{n,j}$ denotes the distance from the n th EV to the j th charging station, and N_G denotes the number of charging stations. Thus, $R_{n,j}$ can be calculated as the sum of road segments in the planned path

$$R_{n,j} = \sum_{k_m \in L_{i,j}} d_{k_m, k_{m+1}}. \quad (8)$$

In an urban transport network, the energy consumption per unit mile of EVs varies greatly under different traffic conditions. We use the speed–energy model [10] to reflect the relationship between energy consumption and traveling speed:

$$\begin{cases} \Delta E_f(t) = 0.247 + \frac{1.52}{\bar{V}_{ij}(t)} - 0.004\bar{V}_{ij}(t) \\ \quad + 2.992 \times 10^{-5} \bar{V}_{ij}(t) \\ \Delta E_m(t) = -0.179 + 0.004\bar{V}_{ij}(t) + \frac{5.492}{\bar{V}_{ij}(t)} \\ \Delta E_{se}(t) = 0.21 - 0.001\bar{V}_{ij}(t) + \frac{1.531}{\bar{V}_{ij}(t)} \end{cases}, \quad (9)$$

where ΔE_f , ΔE_m , and ΔE_{se} are the energy consumption per unit mile for urban expressways, main roads, and secondary roads, respectively. Then, the traveling energy consumption of the n th EV to the j th charging station is found:

$$\Delta E_{n,j} = \sum_{k_m \in L_{i,j}} d_{k_m, k_{m+1}} * \Delta E_{i,j}(t). \quad (10)$$

Based on the driving energy consumption, we can use the remaining SoC of the vehicle to determine its reachable range. The candidate set Sol_n is given by

$$Sol_n = \{j | \Delta E_{n,j} \leq B_{ini,n}^{t_0}\}. \quad (11)$$

Finally, the time cost for the n th EV to the j th charging station in its candidate set, denoted as $T_{n,j}^r$, can be calculated.

2.2.2. Cost of Queuing Time

Assume that the n th EV makes a request for charging at the moment t_0 . The user is not only concerned about the traveling time but also the estimated queuing time. When the EV arrives at the charging station, if the charging piles are fully occupied, it has to wait and start queuing. When any of the charging piles is free, then the EV is able to start charging. When the number of vehicles at the charging station increases, the queuing time will be correspondingly increased. Therefore, the queuing length is also critical for users. In practice, there may be a situation where a vehicle submits a charging request earlier, but it is far away from the charging station. Then, the actual arrival time at the charging station is later than the vehicle that submitted the request later. Therefore, the charging station adopts the principle of "first come, first serve". When the n th EV makes a request for charging at the moment t_0 , the vehicle's position will be sent to the dispatch center. Assuming that the EV is going to the j th charging station for charging, the road traveling time to reach the j th charging station is calculated by the road network model $T_{n,j}^r$. The vehicle arrival time $t_{n,j}^{arr}$ can be calculated as

$$t_{n,j}^{arr} = t_0 + T_{n,j}^r \quad (12)$$

The arrival time of the EV at the charging station and the start of charging time satisfy the following:

$$t_{n,j}^s = t_{n,j}^{arr} + T_{n,j}^w \quad (13)$$

where $T_{n,j}^w$ denotes the waiting time at the j th charging station, and it can be determined as follows:

- When the n th EV arrives at the j th station at $t_{n,j}^{arr}$, if there are no vehicles waiting in line ahead and at least one of charging piles is free, $T_{n,j}^w$ is zero.
- When the n th EV arrives at the j th station at $t_{n,j}^{arr}$, if all charging piles are occupied so that vehicle should enter the queue and charge in turn, then $T_{n,j}^w$ is above zero.

2.2.3. Cost of Charging Time

When the vehicle accesses the charging pile to start charging, the charging time is determined by the charging rate and the remaining SoC. We refer to the charging rate curve in Ref. [24] to calculate the time required for the vehicle to be fully charged, as shown in Figure 3. The remaining SoC $B_{arr_{n,j}}$ when n th EV arrives at the j th charging station can be calculated as

$$B_{arr_{n,j}} = B_{ini_n}^{t_0} - \Delta E_{n,j}, \quad (14)$$

where $B_{ini_n}^{t_0}$ is the n th EV's initial state of charge when it sends the charging request at time t_0 , and $\Delta E_{n,j}$ is its energy consumption on the road to the j th charging station. Then, $B_{arr_{n,j}}$ is substituted into the charging curve to calculate the charging time $T_{n,j}^{ch}$. The relationship between $T_{n,j}^{ch}$ and $B_{arr_{n,j}}$ satisfies

$$SOC(t) = 1.0 + xe^{-yt} - (1+k)e^{-zt}, \quad (15)$$

$$B_{arr_{n,j}} = SOC(t_{arr_{n,j}}), \quad (16)$$

$$T_{n,j}^{ch} = T_{full} - t_{arr_{n,j}}. \quad (17)$$

In the above equations, x , y , and z are the scale coefficients of the charging process. $t_{arr_{n,j}}$ denotes the time required for the vehicle to charge from 0% to $B_{arr_{n,j}}$. T_{full} is the time required for the vehicle to charge from 0% to 100%. In this paper, we set T_{full} as a fixed value.

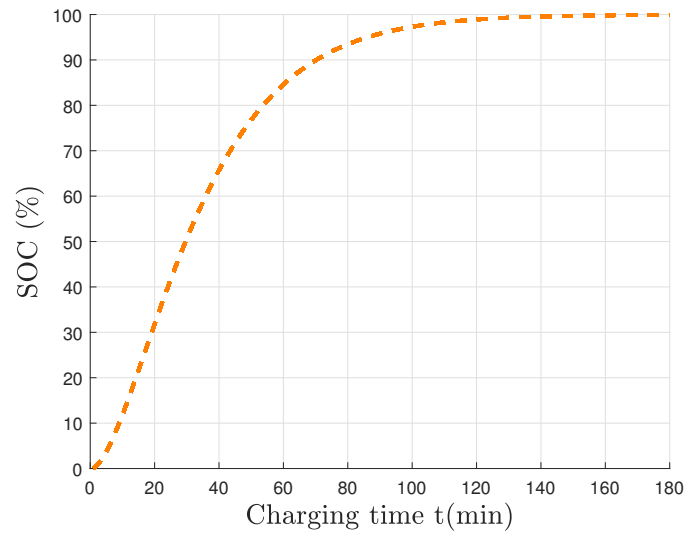


Figure 3. The charging curve of battery.

Through the above calculation, we can obtain the arrival time, residence time, and departure time of the n th EV if it selects the j th charging station.

2.2.4. Cost of Total Time

Based on the above information, we calculate the total time cost $T_{n,j}^{all}$ as

$$T_{n,j}^{all} = T_{n,j}^r + T_{n,j}^w + T_{n,j}^{ch}. \tag{18}$$

Figure 4 shows the detailed time costs.

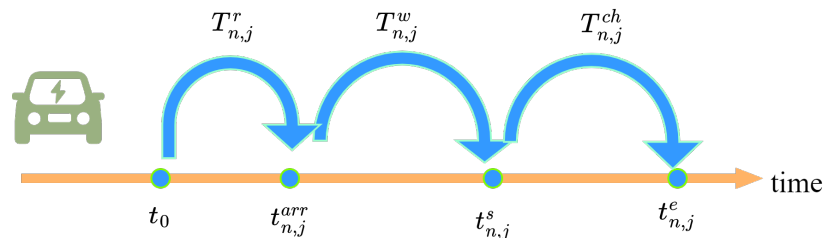


Figure 4. The time cost of a vehicle.

2.3. Spatial Load Balancing

From the user’s points, they naturally tend to choose the charging station with the lowest time cost. However, if a large amount of users select the same charging station at the same time, then the charging load of this charging station will be very high, which dramatically increases the load of the MG where this charging station is located. If the above situation coincides with the peak load of the MG, the gap between different MGs will be enlarged, which further increases the risk of MMG operation. To deal with the problem, we introduce the concept of spatial load balancing to alleviate the problem of large load difference between MGs.

Assuming that the n th EV charges at the j th charging station, it will increase the load of the j th MG during its charging period. Denote the average of updated load of j th MG during the charging period as

$$\overline{P}_{n,j} = \frac{1}{T_{n,j}^{ch}} \sum_{t=t_{n,j}^s}^{t_{n,j}^s+T_{n,j}^{ch}} P_j(t), t \in [t_{n,j}^s, t_{n,j}^s + T_{n,j}^{ch}], \tag{19}$$

where $T_{n,j}^{ch}$ denotes the length of the corresponding charging period, and $P_j(t)$ is the load of the MG at t with the consideration of the EV charging. A good scheduling strategy should guide vehicles to the charging station located at the MG with low load so as to achieve the purpose of 'peak load shifting' and alleviate load difference between MGs.

3. Selection of the Best Charging Station

In the above analysis, we not only consider the time cost of users, but we also study the impact of EV charging activities on the average load of MMG. In order to take into account the dual needs of users' cost and MMG stability, we use the entropy weight method to achieve the purpose of joint optimization. Specifically, we define an optimization model that contains multiple weighting coefficients that reflect the relative importance between users' cost and MMG impact. By adjusting these weighting coefficients, we can flexibly balance the relationship between users' cost and MMG load. Through this method, we hope to establish a more flexible and efficient EV charging scheduling framework to maintain the efficient operation and reliability of MMG. The entropy weight method is an objective weighting method based on information entropy, which is used to determine the weight of each index in multi-index evaluation. The specific steps are as follows:

(1) Data standardization

Due to the different dimensions of different indicators, it is necessary to normalize the data to the [0, 1] interval. For the negative index (the smaller the better), the reverse normalizing formula is

$$x'_{ij} = \frac{\max(x_i) - x_{ij}}{\max(x_i) - \min(x_i)} \quad (20)$$

where x_{ij} defines the original data, and x'_{ij} defines the normalized data.

(2) Calculate the proportion of indicators

Calculate the proportion of the j th index in the i th sample:

$$p_{ij} = \frac{x'_{ij}}{\sum_{i=1}^u x'_{ij}} \quad (21)$$

Among them, p_{ij} is the proportion of the j th index in the i th sample, and u is the number of samples.

(3) Calculation of information entropy

Calculate the information entropy of the j th index:

$$e_j = -h \sum_{i=1}^u p_{ij} \ln(p_{ij}). \quad (22)$$

Here, $h = \frac{1}{\ln(u)}$ is a constant, which is used to ensure that the value of information entropy is between [0, 1].

(4) Calculate the difference coefficient

Calculate the difference coefficient of the j th index:

$$g_j = 1 - e_j. \quad (23)$$

(5) Calculate the weight

The weight of the j th index is calculated according to the difference coefficient:

$$w_j = \frac{g_j}{\sum_{j=1}^s g_j}, \quad (24)$$

where w_j is the weight of the j th index, and s is the number of indicators.

Suppose that the time cost of users and the average load of the j th MG are recorded as $T_{n,j}$ and $P_{n,j}$, respectively. After normalization, they are recorded as $T'_{n,j}$ and $P'_{n,j}$. Then, we calculate the weights w_1 and w_2 of $T'_{n,j}$ and $P'_{n,j}$ by using entropy weight method so as to combine two parts into a parameter:

$$C_{n,j} = w_1 * T'_{n,j} + w_2 * P'_{n,j}. \quad (25)$$

In the MTC-SLBMS model, EVs select the best charging station with comprehensive index for the time cost and spatial load balancing among the candidate solutions. The vehicle dispatch center selects the appropriate charging station j th for the i th EV according with the following rules:

$$j = \operatorname{argmin}(C_{n,1}, \dots, C_{n,j}, \dots), j \in \operatorname{Sol}_n \quad (26)$$

$$\text{s.t. } \operatorname{Sol}_n = \{j | \Delta E_{n,j} \leq B_{ini_n}^{t_0}\} \quad (27)$$

$$w_1 + w_2 = 1. \quad (28)$$

The algorithm flowchart is shown in Figure 5. In this way, the MTC-SLBMS combines the dual considerations of time cost and spatial load balancing, which enhances the charging experience of EV users and the stability of the MMG.

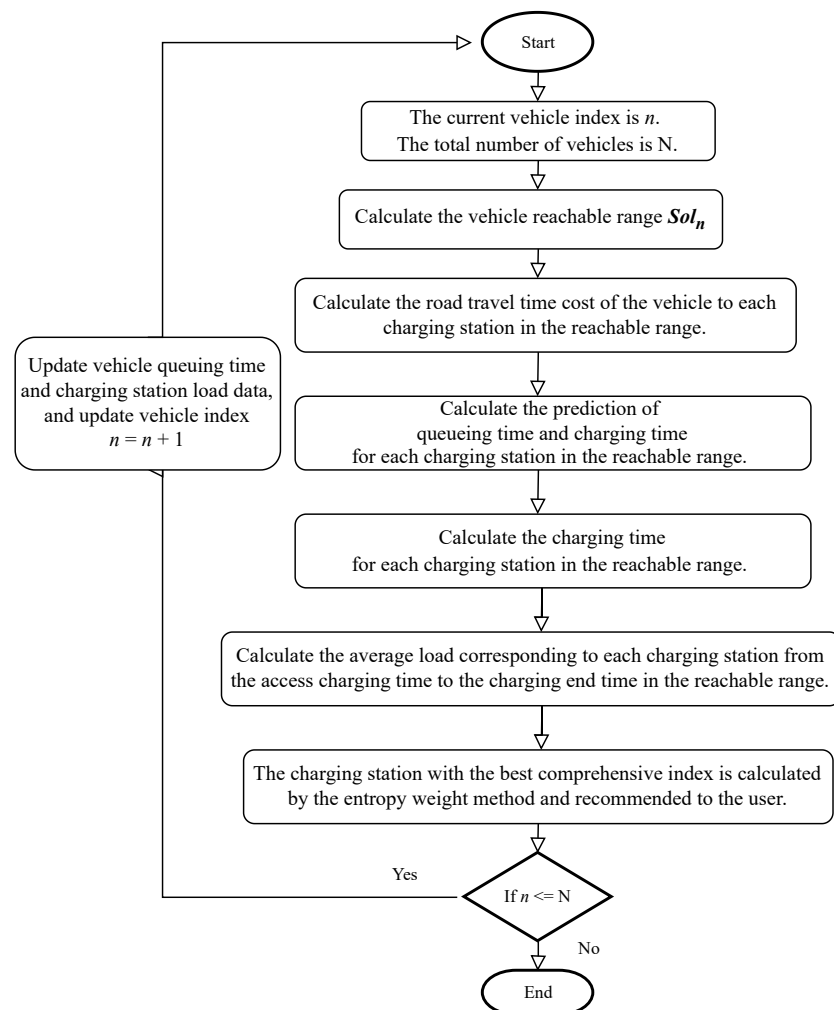


Figure 5. MTC-SLBMS algorithm flowchart.

4. Simulation and Analysis

This section presents the simulation setup and results. We analyze the performance of the proposed method and validate its effectiveness.

4.1. Parameter Setting

Taking the 34-node traffic network in Ref. [11] as an example, the feasibility of the new scheduling strategy is verified. The network size is 20 km × 20 km. The region contains 34 road network nodes and 54 road sections. The area is divided into 7 MGs, and each MG contains a charging station, as shown in Figure 6. The program runs on a computer configured as i7-9700, and the simulation platform is MATLAB. The simulation settings are as follows:

- The initial load data used in the simulation come from the actual data of California's power demand [32]. After scaling down, the data are randomly assigned to the charging stations. The sampling interval of the data is 5 min. In the simulation, the total number of time slots $T_d = 288$, and the sampling time window is 0:00–23:55. All EVs issue charging requests in chronological order during this time window.
- According to Ref. [10], for urban expressways, a , b , and m in Formula (3) are 1.726, 3.15, and 3, respectively; for the main road and the secondary road, a , b , and m are 2.076, 2.870, and 3, respectively. $\bar{V}_{ij}^{free} = 60$ km/h.
- The number of charging piles in each charging station C is set to 50 unless otherwise specified.
- Other parameter settings are shown in Table 1.

The traffic conditions of the road traffic network at some typical moments are shown in Figure 7.

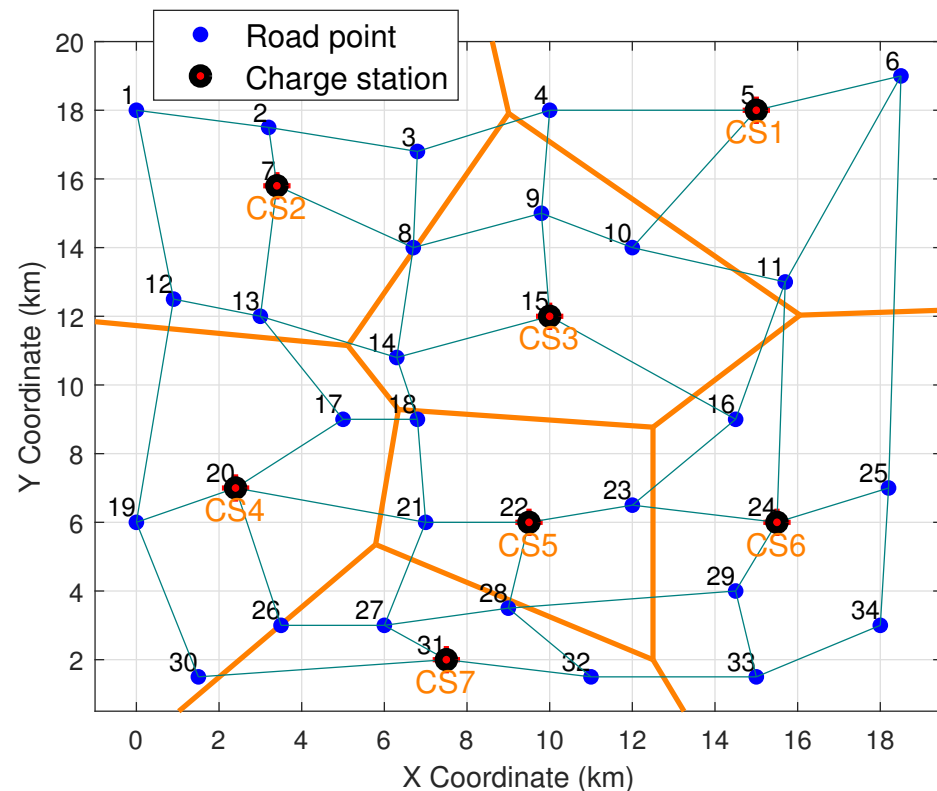


Figure 6. Road network.

of the MMG. We use the average time cost of users \bar{T} to measure the user's time cost under different strategies. The definition of \bar{T} is as follows:

$$\bar{T} = \frac{\sum_{n=1}^N (T_{n,j}^r + T_{n,j}^w + T_{n,j}^{ch})}{N}. \quad (29)$$

In order to measure the load balance between MGs at time t , the valley-to-peak ratio $\eta(t)$ is used as the performance index:

$$\eta(t) = \frac{P_{valley}(t)}{P_{peak}(t)} \times 100\%, \quad (30)$$

where $P_{valley}(t)$ and $P_{peak}(t)$ are the lowest and highest loads of MGs at time t , respectively. The larger the value of $\eta(t)$, the smaller the valley-peak gap between MGs at time t , which is conducive to the operation of the power grid. On this basis, we define the average valley-to-peak ratio $\bar{\eta}$ to measure the load balance between MGs in the entire sampling window. $\bar{\eta}$ is defined as

$$\bar{\eta} = \frac{1}{T_d} \sum_{t=1}^{T_d} \eta(t). \quad (31)$$

We introduced a new composite index (CI), which is obtained by normalizing the "average time cost" and the "average valley-to-peak ratio" separately and then summing them. For \bar{T} , lower values are preferable, so we applied the reverse normalization method. For $\bar{\eta}$, higher values are better, so we applied forward normalization method. The formula is as follows:

$$\bar{T}' = \frac{\max(\bar{T}) - \bar{T}}{\max(\bar{T}) - \min(\bar{T})} \quad (32)$$

$$\bar{\eta}' = \frac{\bar{\eta} - \min(\bar{\eta})}{\max(\bar{\eta}) - \min(\bar{\eta})} \quad (33)$$

$$CI = \bar{T}' + \bar{\eta}'. \quad (34)$$

where \bar{T}' is the value obtained by reverse normalizing \bar{T} , and $\bar{\eta}'$ is the value obtained by forward normalizing $\bar{\eta}$.

4.3. Strategies for Comparison

We will compare our proposed strategy with the following ones.

4.3.1. SDMS

In the Shortest Distance Matching Strategy (SDMS), EVs select the nearest charging station among the candidate solutions. In this strategy, the vehicle dispatch center selects the appropriate charging station for the n th EV according to the following rules:

$$j = \operatorname{argmin}(R_{n,j}), j \in \operatorname{Sol}_n. \quad (35)$$

The SDMS is beneficial to EV users because it can save them time. However, as an uncertain load in the power grid, the disorderly charging behaviors of EVs bring a burden to the power grid to a certain extent. Although the SDMS can well meet the time requirement of EV users, it cannot make full use of the characteristics of EVs as the load balancing tool in power system. If a large number of EVs choose the same charging station at the same time, this charging behavior may threaten the safe operation of the power system.

4.3.2. TMMS

In the Time Minimum Matching Strategy (TMMS), EVs select the charging stations with the shortest charging time among the candidate solutions. In this strategy, the vehicle dispatch center selects the appropriate charging station for the n th EV according to the following rule:

$$j = \operatorname{argmin}(T_{n,j}^{all}), j \in \operatorname{Sol}_n. \quad (36)$$

The TMMS considers the traffic flow of roads and the congestion of charging stations to minimize their charging time.

4.3.3. LBMS

Chen et al. [24] proposed the Load Balancing Matching Strategy (LBMS). In the LBMS, EVs select charging stations with the lowest load at the time when the EV makes a request to charge. In this strategy, the vehicle dispatch center selects the appropriate charging station for the n th EV according to the following rule:

$$j = \operatorname{argmin}(P_j(t_0)), j \in \operatorname{Sol}_n. \quad (37)$$

The LBMS is conducive to the stability of power system, because it can balance the load of each charging station and reduce the risk of overload of the MG. However, this strategy may lead to higher time costs for EV users, thus affecting their charging experience.

4.3.4. ILBMS

Xia et al. [26] proposed the Improved Load Balancing Matching Strategy (ILBMS). In the ILBMS, the EV selects the charging station with the lowest average load during its charging process. In this strategy, the vehicle dispatch center selects the appropriate charging station for the n th EV according to the following rule:

$$j = \operatorname{argmin}(\overline{P}_{n,j}), j \in \operatorname{Sol}_n. \quad (38)$$

Compared to the LBMS, the ILBMS considers load fluctuation during the EV's charging period so that the effect of spatial load balancing is better defined. However, the ILBMS still does not consider the charging experience of EV users, and the time cost of users is still high.

4.4. Analysis of Performance

In order to verify the performance of the MTC-SLBMS, we simulated and analyzed EV scheduling and charging processes based on the above strategies. Figures 8 and 9 compare the average time cost of users and average valley-to-peak ratio with the increasing number of vehicles under different strategies. From those figures, we observe that the SDMS and TMMS algorithms did provide the lowest average time cost of users, but their main flaw is imbalanced load distribution, as their respective valley-to-peak ratio outputs are extremely low. On the contrary, although the LBMS and ILBMS algorithms performed well in balancing load of MMG system, they led to a significant increase in the time cost of users. Although the proposed MTC-SLBMS algorithm did not perform the best on either the time cost of users or the valley-to-peak ratio, its performance was quite close to the best one and much better than the worst ones in both figures. Therefore, taking both aspects of performance into account, the MTC-SLBMS algorithm can achieve the best comprehensive performance.

In Figure 10, we compare the composite index (CI) across different scheduling strategies. Figure 10 illustrates the comparison of the composite index under various strategies for different vehicle numbers N with a fixed charging station capacity of $C = 50$. The bar chart

displays the performance of five different strategies: the SDMS, TMMS, LBMS, ILBMS, and MTC-SLBMS. As the number of vehicles changed, the MTC-SLBMS consistently achieved the highest value, indicating the effectiveness of our method in optimizing both user time cost and spatial load balancing between MMGs.

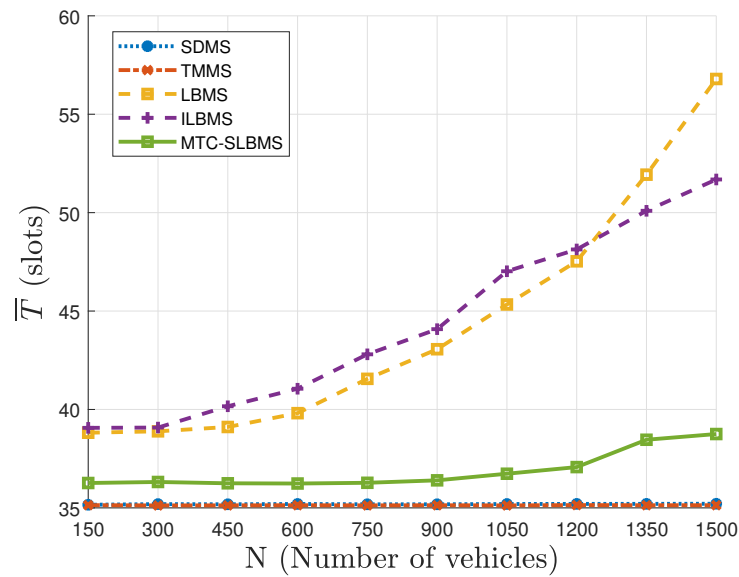


Figure 8. Comparison of average time cost under different strategies ($C = 50$).

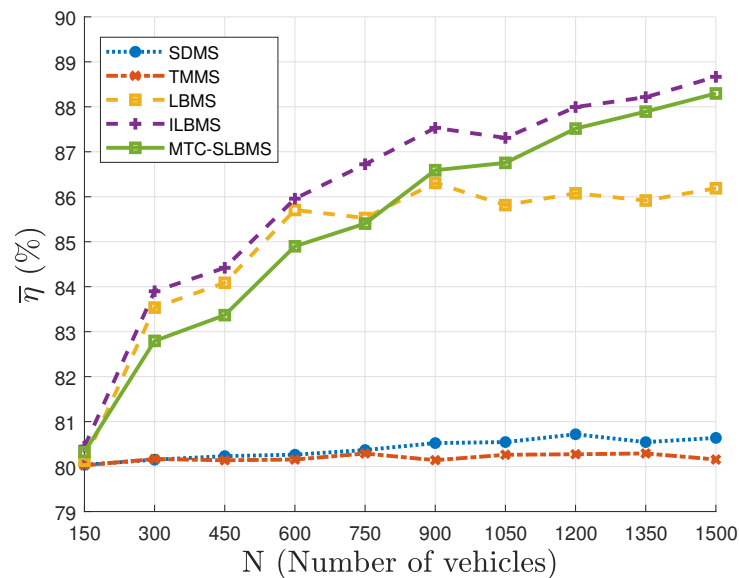


Figure 9. Comparison of average valley-to-peak ratio under different strategies ($C = 50$).

Table 2 presents the composite index values under different microgrid scales (5 MGs, 7 MGs, and 9 MGs), with a fixed number of vehicles at $N = 1500$ and charging station capacity of $C = 50$. The composite index values are listed for different scales, highlighting the advantage of the proposed MTC-SLBMS strategy compared to other methods. As shown, the MTC-SLBMS consistently outperformed the other strategies across all scales, demonstrating its superiority in terms of both load balancing and optimization of user time cost. These results emphasize the effectiveness and scalability of the MTC-SLBMS approach, particularly in managing larger-scale microgrids and varying numbers of vehicles.

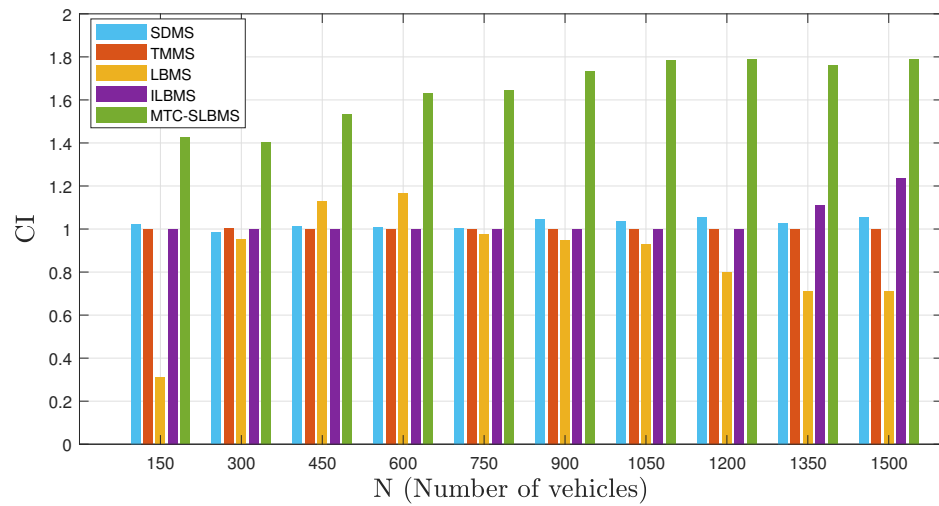


Figure 10. Comparison of composite index(CI) under different strategies (C = 50).

Table 2. Composite index(CI) under different MMG scales (N = 1500 and C = 50).

	5 MGs	7 MGs	9 MGs
SDMS	1.176	1.053	1.070
TMMS	1	1	1
LBMS	0.407	0.709	0.851
ILBMS	1.541	1.236	1.376
MTC-SLBMS	1.763	1.790	1.768

Figure 11 shows the variation of the average valley-to-peak ratio $\bar{\eta}$ as the number of vehicles N increased for different levels of user participation. The graph illustrates three scenarios: 0% participation, 50% participation, and 100% participation. This figure highlights the positive correlation between user participation and the effectiveness of load balancing, showing that greater user involvement results in improved system performance, particularly in terms of load distribution across MMGs. The increasing trend suggests that optimizing user participation can significantly enhance the system’s efficiency.

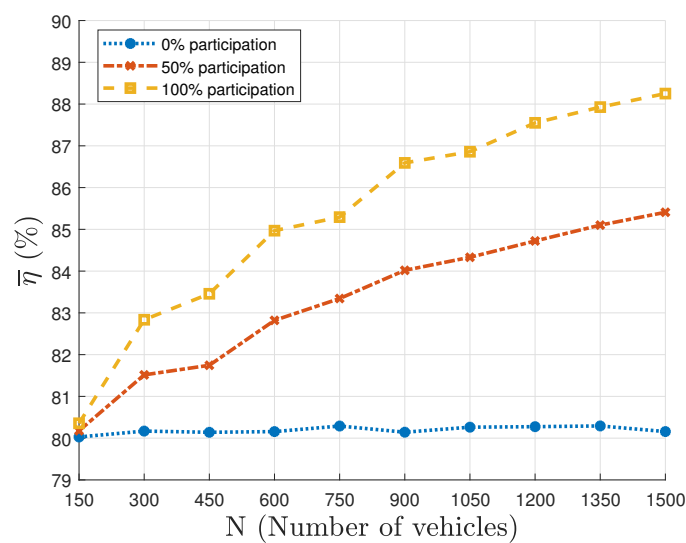


Figure 11. Average valley-to-peak ratio under different participation (C = 50).

Take the first MG as a case study. Figure 12 illustrates the load curve under different EV charging scheduling strategies. There are 1500 EVs in the simulation, and the capacity

of each charging station is $C = 50$. The SDMS and TMMS primarily enhanced charging efficiency by minimizing distance and time cost, respectively. However, as we can see in the figure, these two strategies evenly added almost the same charging load to the initial load, no matter in peak hour or valley. In this way, these strategies overlook the fluctuating demand and real-time load conditions on an MG. That is why their performance in load balancing was quite poor. The LBMS and ILBMS strategies are designed primarily to stabilize the power system by optimizing load distributions among MGs. Upon observing the curves in the figure, the MTC-SLBMS strategy also achieved a commendable load balancing effect.

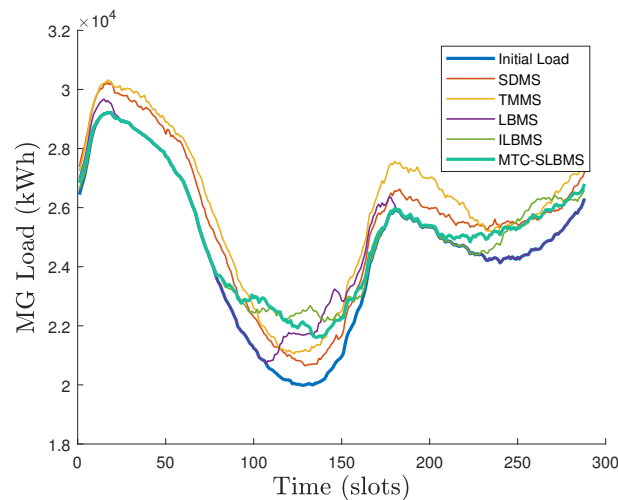


Figure 12. MG load curve under different strategies ($N = 1500$ and $C = 50$).

Figure 13 illustrates the distribution of vehicles across different charging stations under various strategies. A critical issue with EV charging is that when a large number of vehicles converge in a single charging station, this can cause significant congestion, leading to substantially increased waiting times for users. This not only impacts user satisfaction but also reduces the overall efficiency of the charging infrastructure. In the LBMS and ILBMS, while efforts are made to balance the grid load, they often fall short in addressing the uneven distribution of vehicles across charging stations. This will make some stations overloaded so that the waiting time will be extended. By considering not only the spatial distribution of grid load but also the time cost of EVs charging, the MTC-SLBMS ensures a more even distribution of vehicles across charging stations than the LBMS and ILBMS do.

Then, the performance of the MTC-SLBMS algorithm under different charging station capacities was explored. The capacity of a charging station, defined by the number of available charging piles, is a critical factor influencing the efficiency of EVs charging operations. This capacity directly impacts not only the average time cost for users but also the overall load management within the power system. When the number of charging piles is large, the system can handle a higher influx of vehicles without significant delays. This not only reduces the waiting time for individual users but also allows more vehicles to be charged in MGs with low initial load, thereby increasing the valley-to-peak ratio. This effect is beneficial for the grids, as it smooths out fluctuations. On the other hand, when the capacity is low, the system becomes more prone to congestion. As the queue of waiting vehicles grows, the start times for charging are delayed, which means that the time cost for users increases. At the same time, the low capacity diminishes the “valley filling” effect, where ideally, vehicles would charge during the troughs in power demand to balance the load. As a result, the effectiveness of load balancing diminishes, leading to potential peaks during higher demand periods and less efficient use of the grid’s capacity.

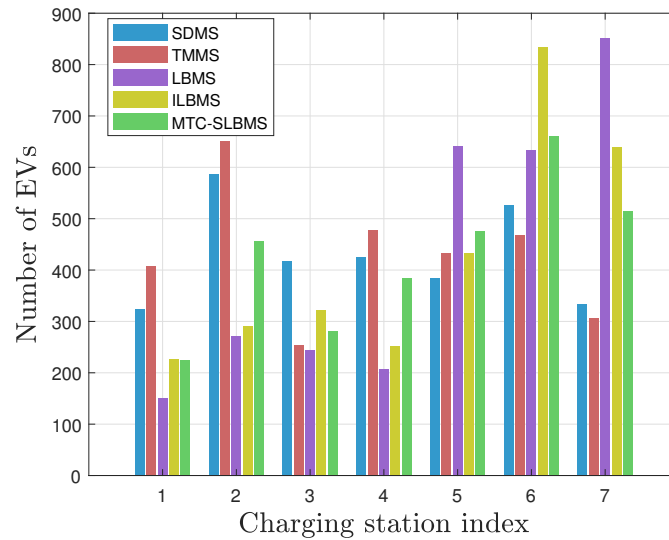


Figure 13. Comparison of the number of vehicles in each charging station under different strategies (C = 50).

Figures 14 and 15 illustrate these dynamics by comparing how the average time cost and average valley-to-peak ratio change with increasing numbers of vehicles under different station capacities. As seen in Figure 14, with higher capacity, the system proved to be better equipped to handle increased demand, resulting in reduced time costs for users. Figure 15 shows that the increase in the number of vehicles contributes positively to the valley-to-peak ratio. However, with a low capacity, the demand is easier to surpass the station’s capacity, then this positive effect is weakened, leading to a slowdown in the growth rate of the curve.

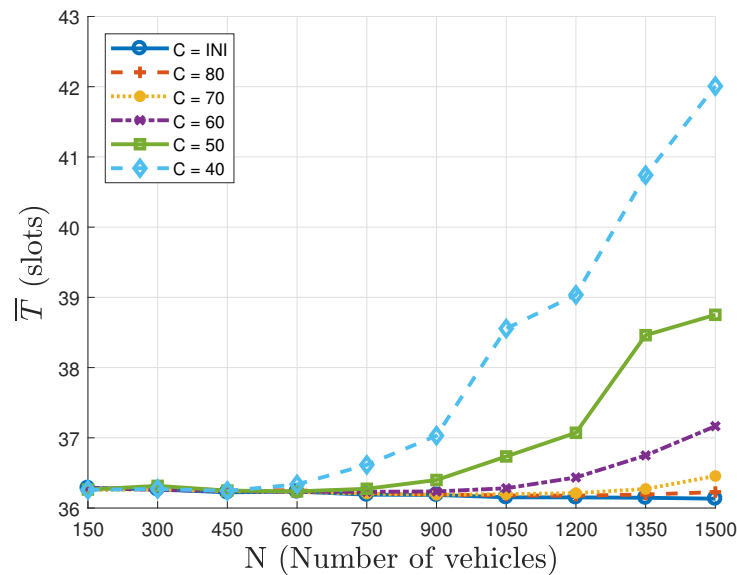


Figure 14. Comparison of average time cost under different charging station capacities.

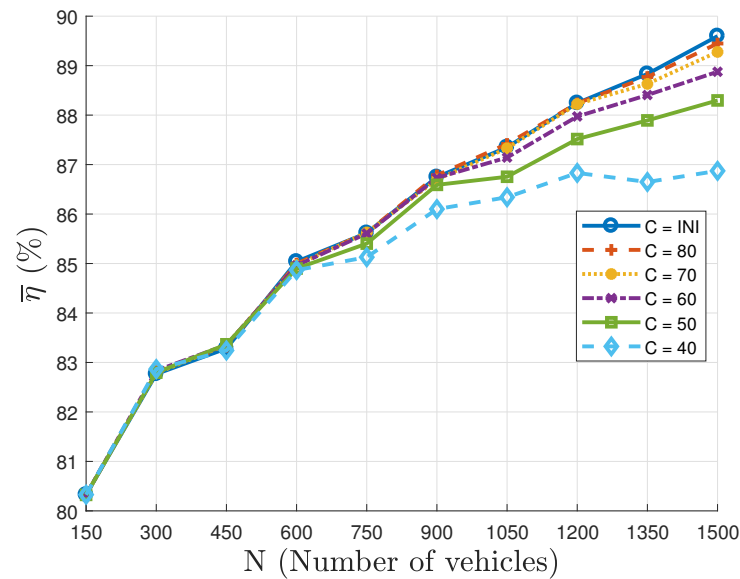


Figure 15. Comparison of average valley-to-peak ratio under different charging station capacities.

5. Conclusions and Future Work

In this paper, we established an EV charging network model that consists of an MMG and a traffic network. From the dual perspective of users and MMG, the charging time cost of users and the load fluctuation of MMG have been comprehensively considered. We proposed a novel scheduling strategy, the MTC-SLBMS, to minimize users' time costs while optimizing spatial load balancing among MMGs. The simulation results show that, compared to the SDMS and the TMMS methods, our approach improved the average peak-to-valley ratio by 9.5% and 10.2%, respectively. Similarly, compared to the LBMS and the ILBMS methods, our approach reduced the average time cost by 31.8% and 25% while maintaining satisfactory spatial load balancing. It retained the advantages of both the SDMS/TMMS and LBMS/ILBMS while overcoming their limitations, offering a more comprehensive solution. In addition, we explored the performance of the proposed MTC-SLBMS method under different MMG scales, different user participation, and different charging station capacities, and we verified the feasibility of the method in many aspects, making the conclusion more universal.

Our method relies on real-time data, which requires significant computational resources to process. Given the reliance on accurate and timely data inputs, any delays or inaccuracies could potentially affect system performance. To address this, future research could incorporate advanced technologies such as edge computing and cloud computing to enhance computational power, enabling more efficient scheduling decisions. These technologies would support the development of smart cities by improving the data transmission speed between vehicles and the scheduling center. Additionally, integrating data prediction models could improve the accuracy of the forecasted data, helping to ensure that the scheduling strategy remains stable and effective.

Author Contributions: Conceptualization, J.Z., Y.X., Z.C., and X.C.; methodology, J.Z., Y.X., Z.C., and X.C.; software, J.Z.; validation, J.Z.; formal analysis, J.Z.; investigation, J.Z.; resources, J.Z.; data curation, J.Z.; writing—original draft preparation, J.Z.; writing—review and editing, Y.X., and X.C.; visualization, J.Z.; supervision, Y.X., Z.C., and X.C.; project administration, J.Z., and Y.X. All authors have read and agreed to the published version of the manuscript.

Funding: This research received no external funding.

Data Availability Statement: The data presented in this study are not publicly available due to privacy concerns.

Conflicts of Interest: The authors declare no conflicts of interest.

Abbreviations

The following abbreviations are used in this manuscript:

EVs	Electric Vehicles
MG	Microgrid
MMG	Multi-Microgrid
V2G	Vehicle To Grid
LBMS	Load Balancing Matching Strategy
MTC-SLBMS	Minimum Time Cost–Spatial Load Balancing Matching Strategy
SoC	State Of Charge
SDMS	Shortest Distance Matching Strategy
TMMS	Time Minimum Matching Strategy
ILBMS	Improved Load Balancing Matching Strategy

Nomenclature

V	The number of road nodes.
E	The number of connected road segments.
D	The matrix of road weight.
d_{ij}	The distance from point i to point j (km).
e_{ij}	The road section from point i to point j .
$\bar{V}_{ij}(t)$	The average speed of the road section e_{ij} (km/h).
$q_{ij}(t)$	The traffic flow of the road section e_{ij} (Number of vehicles/h).
$C_{ij}(t)$	The capacity of the road section e_{ij} (Number of vehicles/h).
$a, b, \text{ and } m$	The adaptive coefficients for different road levels.
T	The matrix of time weight.
t_{ij}	The time from point i to point j (slots).
t_0	The request time of the EV.
$B_{ini,n}^{t_0}$	The initial SoC of the n th EV at time t_0 (%).
$L_{i,j}$	The sequence of the shortest path.
$R_{n,j}$	The distance from the n th EV to the j th charging station (km).
N_G	The number of charging stations.
$\Delta E_{n,j}$	The traveling energy consumption of the n th EV to the j th charging station (%).
Sol_n	The candidate set of the vehicle reachable range.
$T_{n,j}^r$	The road traveling time of the n th EV to reach the j th charging station (slots).
$t_{n,j}^{arr}$	The arrival time of the n th EV to reach the j th charging station.
$T_{n,j}^w$	The waiting time of the n th EV at the j th charging station (slots).
$t_{n,j}^s$	The start charging time of the n th EV at the j th charging station.
$x, y, \text{ and } z$	The scale coefficients of the charging process.
$T_{n,j}^{ch}$	The charging time of the n th EV at the j th charging station (slots).
$t_{n,j}^e$	The end charging time of the n th EV at the j th charging station.
$P_j(t)$	The load of the j th MG at time t (kWh).
$\bar{P}_{n,j}$	The average load of the j th MG during the n th EV's charging period (kWh).
$T_{n,j}$	The time cost of the n th EV at the j th charging station (slots).
$T'_{n,j}$	Normalized the time cost of the n th EV at the j th charging station.
$P'_{n,j}$	Normalized the average load of the j th MG during the n th EV's charging period.
$w_1 \text{ and } w_2$	The weights of $T'_{n,j}$ and $P'_{n,j}$ using the entropy weight method.
$C_{n,j}$	The comprehensive value of both the time cost and the average load assuming that the n th EV go to the j th charging station.

p	The charging power of an EV at the charging station (kWh).
R_{max}	The maximum driving distance of EVs (km).
T_{full}	The time required for the vehicle to charge from 0% to 100% (slots).
N	The total number of EVs.
\bar{T}	The average time cost of users (slots).
$\bar{\eta}$	The average valley-to-peak ratio among MMGs (%).
\bar{T}'	Normalized time cost of users.
$\bar{\eta}'$	Normalized average valley-to-peak ratio among MMGs.
CI	The comprehensive index of both the average time cost and the average valley-to-peak ratio.

References

1. Tse, C.K.; Huang, M.; Zhang, X.; Liu, D.; Li, X.L. Circuits and systems issues in power electronics penetrated power grid. *IEEE Open J. Circuits Syst.* **2020**, *1*, 140–156. [\[CrossRef\]](#)
2. Xu, Y.; Çolak, S.; Kara, E.C.; Moura, S.J.; González, M.C. Planning for electric vehicle needs by coupling charging profiles with urban mobility. *Nat. Energy* **2018**, *3*, 484–493. [\[CrossRef\]](#)
3. Wang, D.; Locment, F.; Sechilariu, M. Modelling, simulation, and management strategy of an electric vehicle charging station based on a DC microgrid. *Appl. Sci.* **2020**, *10*, 2053. [\[CrossRef\]](#)
4. Sayed, K.; Abo-Khalil, A.G.; Alghamdi, A.S. Optimum resilient operation and control DC microgrid based electric vehicles charging station powered by renewable energy sources. *Energies* **2019**, *12*, 4240. [\[CrossRef\]](#)
5. Wu, C.; Jiang, S.; Gao, S.; Liu, Y.; Han, H. Charging demand forecasting of electric vehicles considering uncertainties in a microgrid. *Energy* **2022**, *247*, 123475. [\[CrossRef\]](#)
6. Li, Z.; Sun, Y.; Anvari-Moghaddam, A. A consumer-oriented incentive mechanism for EVs charging in multi-microgrids based on price information sharing. In Proceedings of the 2021 IEEE International Conference on Environment and Electrical Engineering and 2021 IEEE Industrial and Commercial Power Systems Europe (EEEIC/I&CPS Europe), Bari, Italy, 7–10 September 2021; pp. 1–6. [\[CrossRef\]](#)
7. Huang, Z.; Guo, Z.; Ma, P.; Wang, M.; Long, Y.; Zhang, M. Economic-environmental scheduling of microgrid considering V2G-enabled electric vehicles integration. *Sustain. Energy Grids Netw.* **2022**, *32*, 100872. [\[CrossRef\]](#)
8. Wei, Y.; Han, T.; Wang, S.; Qin, Y.; Lu, L.; Han, X.; Ouyang, M. An efficient data-driven optimal sizing framework for photovoltaics-battery-based electric vehicle charging microgrid. *J. Energy Storage* **2022**, *55*, 105670. [\[CrossRef\]](#)
9. Elghitani, F.; El-Saadany, E.F. Efficient assignment of electric vehicles to charging stations. *IEEE Trans. Smart Grid* **2021**, *12*, 761–773. [\[CrossRef\]](#)
10. Li, X.; Xiang, Y.; Lyu, L.; Ji, C.; Zhang, Q.; Teng, F.; Liu, Y. Price incentive-based charging navigation strategy for electric vehicles. *IEEE Trans. Ind. Appl.* **2020**, *56*, 5762–5774. [\[CrossRef\]](#)
11. Xiang, Y.; Yang, J.; Li, X.; Gu, C.; Zhang, S. Routing optimization of electric vehicles for charging with event-driven pricing strategy. *IEEE Trans. Autom. Sci. Eng.* **2022**, *19*, 7–20. [\[CrossRef\]](#)
12. Ji, C.; Liu, Y.; Lyu, L.; Li, X.; Liu, C.; Peng, Y.; Xiang, Y. A personalized fast-charging navigation strategy based on mutual effect of dynamic queuing. *IEEE Trans. Ind. Appl.* **2020**, *56*, 5729–5740. [\[CrossRef\]](#)
13. Shi, L.; Zhan, Z.-H.; Liang, D.; Zhang, J. Memory-based ant colony system approach for multi-source data associated dynamic electric vehicle dispatch optimization. *IEEE Trans. Intell. Transp. Syst.* **2022**, *23*, 17491–17505. [\[CrossRef\]](#)
14. Rasheed, M.B.; Awais, M.; Alquthami, T.; Khan, I. An optimal scheduling and distributed pricing mechanism for multi-region electric vehicle charging in smart grid. *IEEE Access* **2020**, *8*, 40298–40312. [\[CrossRef\]](#)
15. Sweda, T.M.; Klabjan, D. Finding minimum-cost paths for electric vehicles. In Proceedings of the 2012 IEEE International Electric Vehicle Conference, Greenville, SC, USA, 4–8 March 2012; pp. 1–4. [\[CrossRef\]](#)
16. Jia, Y.H.; Mei, Y.; Zhang, M. A bilevel ant colony optimization algorithm for capacitated electric vehicle routing problem. *IEEE Trans. Cybern.* **2022**, *52*, 10855–10868. [\[CrossRef\]](#)
17. Liu, Y.; Wang, Y.; Li, Y.; Gooi, H.B.; Xin, H. Multi-agent based optimal scheduling and trading for multi-microgrids integrated with urban transportation networks. *IEEE Trans. Power Syst.* **2021**, *36*, 2197–2210. [\[CrossRef\]](#)
18. Phommixay, S.; Doumbia, M.L.; Lupien St-Pierre, D. Review on the cost optimization of microgrids via particle swarm optimization. *Int. J. Energy Environ. Eng.* **2019**, *11*, 73–89. [\[CrossRef\]](#)
19. Zhao, B.; Wang, X.; Lin, D.; Calvin, M.M.; Morgan, J.C.; Qin, R.; Wang, C. Energy management of multiple microgrids based on a system of systems architecture. *IEEE Trans. Power Syst.* **2018**, *33*, 6410–6421. [\[CrossRef\]](#)
20. Shi, J.; Zhang, W.; Bao, Y.; Gao, D.W.; Wang, Z. Load forecasting of electric vehicle charging stations: Attention based spatiotemporal multi-graph convolutional networks. *IEEE Trans. Smart Grid* **2024**, *15*, 3016–3027. [\[CrossRef\]](#)

21. Jian, L.; Zheng, Y.; Shao, Z. High efficient valley-filling strategy for centralized coordinated charging of large-scale electric vehicles. *Appl. Energy* **2017**, *186*, 46–55. [[CrossRef](#)]
22. Kandpal, B.; Pareek, P.; Verma, A. A robust day-ahead scheduling strategy for EV charging stations in unbalanced distribution grid. *Energy* **2022**, *249*, 123737. [[CrossRef](#)]
23. Nimalsiri, N.I.; Ratnam, E.L.; Smith, D.B.; Mediwaththe, C.P.; Halgamuge, S.K. Coordinated charge and discharge scheduling of electric vehicles for load curve shaping. *IEEE Trans. Intell. Transp. Syst.* **2022**, *23*, 7653–7665. [[CrossRef](#)]
24. Chen, X.; Wang, H.; Wu, F.; Wu, Y.; Gonzalez, M.C.; Zhang, J. Multimicrogrid load balancing through EV charging networks. *IEEE Internet Things J.* **2022**, *9*, 5019–5026. [[CrossRef](#)]
25. Gu, X.; Xia, Y.; Fu, D.; Chen, X. Performance under limited service capacity for load balancing EV charging network. *IEEE J. Emerg. Sel. Top. Circuits Syst.* **2023**, *13*, 596–604. [[CrossRef](#)]
26. Xia, Y.; Gu, X.; Fu, D.; Chen, X. Large scale EV charging allocation in unbalanced multi-microgrid system. *IEEE J. Emerg. Sel. Top. Circuits Syst.* **2023**, *13*, 797–805. [[CrossRef](#)]
27. Zhang, X.; Li, P.; Hu, J.; Liu, M.; Wang, G.; Qiu, J.; Chan, K.W. Yen's algorithm-based charging facility planning considering congestion in coupled transportation and power systems. *IEEE Trans. Transp. Electr.* **2019**, *5*, 1134–1144. [[CrossRef](#)]
28. Zhang, K.; Gao, B.; Han, Y.; Dong, Z. Optimization scheduling of electric vehicle charging load based on improved PSO. In Proceedings of 2022 IEEE 2nd International Conference on Mobile Networks and Wireless Communications (ICMNBC), Tumkur, India, 2–3 December 2022; pp. 1–6. [[CrossRef](#)]
29. Luo, Y.; Zhu, T.; Wan, S.; Zhang, S.; Li, K. Optimal charging scheduling for large-scale EV (electric vehicle) deployment based on the interaction of the smart-grid and intelligent-transport systems. *Energy* **2016**, *97*, 359–368. [[CrossRef](#)]
30. Guo, Q.; Xin, S.; Sun, H.; Li, Z.; Zhang, B. Rapid-charging navigation of electric vehicles based on real-time power systems and traffic data. *IEEE Trans. Smart Grid* **2014**, *5*, 1969–1979. [[CrossRef](#)]
31. Zhang, J.; Jing, W.; Lu, Z.; Wu, H.; Wen, X. Collaborative strategy for electric vehicle charging scheduling and route planning. *IET Smart Grid* **2024**, *7*, 628–642. [[CrossRef](#)]
32. California ISO. California ISO Open Access Same-Time Information System. 2020. Available online: <https://www.caiso.com/> (accessed on 10 February 2021).

Disclaimer/Publisher's Note: The statements, opinions and data contained in all publications are solely those of the individual author(s) and contributor(s) and not of MDPI and/or the editor(s). MDPI and/or the editor(s) disclaim responsibility for any injury to people or property resulting from any ideas, methods, instructions or products referred to in the content.